Switching Behavior of Carbon Chains Bridging Graphene Nanoribbons: Effects of Uniaxial Strain

Brahim Akdim*,†,‡ and Ruth Pachter*,†

†Air Force Research Laboratory, Materials & Manufacturing Directorate, AFRL/RX Wright-Patterson Air Force Base, Ohio 45433, United States, and
‡General Dynamics Information Technology Corporation, Dayton, Ohio 45433, United States

ABSTRACT Recently, several experiments demonstrated the stability of chain-like carbon nanowires bridged between graphene nanoribbons, paving the way for potential applications in nanodevices. On the basis of density functional tight-binding calculations, we demonstrated switching for chains terminated with a five-membered ring under an applied strain, serving as a model for morphological changes in realistic materials. Electron transport calculations showed an increase of up to 100% in the output current, achieved at a reverse bias voltage of −2 V and an applied strain of just 1.5%. Structural analysis suggested that the switching is driven by conformational changes, where in our case is triggered by the formation and annihilation of a five-membered ring at the interface of the chain−graphene edge. In addition, we showed that a five-membered ring can easily be formed at the interface under a source−drain bias or through a gate voltage. This mechanism can serve as an explanation of experimentally observed conductance for the materials.

KEYWORDS: density functional theory · non-equilibrium Green's function · electron transport · carbon chains · electrical switching · graphene nanoribbons

Carbon allotropes have long been proposed as post-silicon materials for nanodevice fabrication.[1] Carbon nanotube field-effect transistors (FETs) have been widely demonstrated,[2,3] and the discovery of 2D graphene, robust yet flexible, with unusual electronic properties, also motivated a range of applications.[4−8] For example, FETs with bilayer graphene,[9] or graphene nanoribbons (GNRs) confined to sub-10 nm,[10] were proposed for opening the band gap, thus increasing the ON/OFF ratio of a nanodevice. At the same time, most recently, fabrication of carbon atomic chains from graphene was achieved by controlled electron irradiation in a transmission electron microscope.[11,12] These experiments demonstrated stability of chains with lengths of a few nanometers, hence setting the stage for a new way to produce chain-like structures bridged between GNRs. Interestingly, switching behavior was demonstrated by creating nanoscale gaps,[13] where ON/OFF states were attributed to the formation/annihilation of carbon chains under a 4 V/6 V applied bias. Thus, exploring electrical transport properties of nanodevices based on carbon chains, namely, the carbyne carbon allotrope, already speculated on in 1921,[14] could provide unique opportunities in nanoelectronics.

Carbyne exists in two isomeric forms with different bond length alternation (BLA), that is, cumulene (double bonds) and polyyne (alternating single and triple bonds). This class of materials was recently found to be of interest regarding stabilization upon attachment to sp^2 and sp^3 graphitic nanofragments, in comparison with Raman spectra,[15] or specifically for cumulenes, regarding stability, formation, and unimolecular decomposition.[16] Notably, it was predicted that carbon chains are more stable than small diameter single-wall carbon nanotubes (SWCNTs).[17,18] Previously, aspects of carbon chain conductance were addressed; for example, junctions of carbon chains bridged between SWCNTs were fabricated and studied by first-principles molecular dynamics (MD), showing that a cumulenic structure was stabilized due to a Peierls-like distortion.[19] Earlier theoretical work on the electronic structure of carbon chains[20] explained oscillatory conductance of odd and even chains with metal leads, while investigation by density functional theory (DFT) of a short carbon chain attached to gold electrodes enabled elucidation of the effects of functional groups.[21] DFT calculations also showed changes in the conductance upon doping.[22] Most recently, $I-V$ characteristics of SWCNTs bridged by short carbon chains were studied by DFT,[23] showing qualitative agreement with experiment,[24] also analyzed analytically.[25]

As previously shown, effects of strain can play an important role on the electronic

*Address correspondence to brahim.akdim@wpafb.af.mil, ruth.pachter@wpafb.af.mil.

Received for review September 14, 2010 and accepted February 8, 2011.

Published online February 23, 2011
10.1021/nn102403j

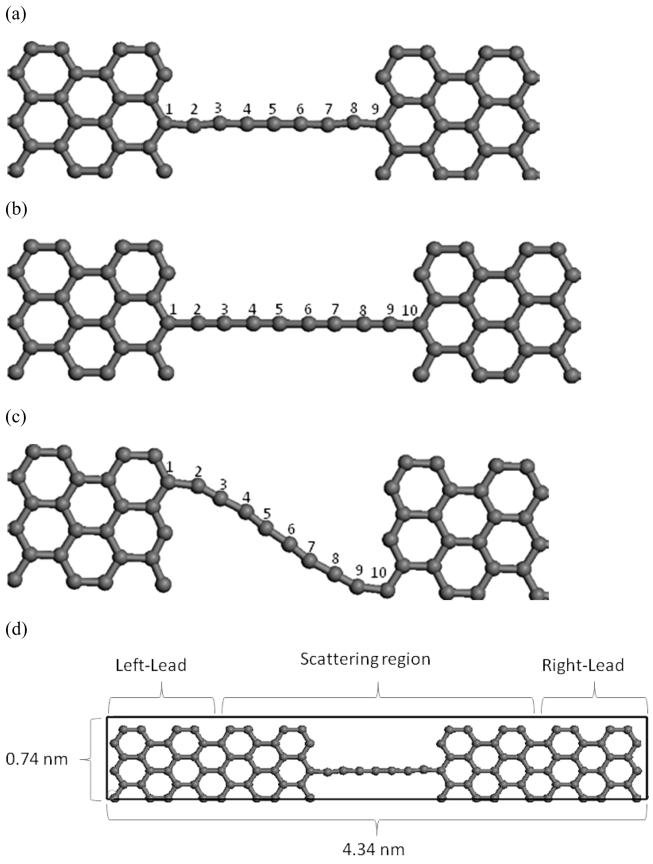

Figure 1. Model structures: C7-CC (a), C8-CC (b), and C8-NCC (c). (d) Zoom-out of the structure of C7-CC, showing the lattice parameters, the leads, and scattering region. The periods of the unit cell were 4.3 and 6.8 nm in the longitudinal and transverse directions, respectively.

properties of carbon nanotubes[26−28] and GNRs in nanodevices.[29] In this work, we explored and demonstrated a switching behavior of carbon chains bridged between GNRs, driven by the formation and annihilation of a five-membered ring at the interface of the carbon chain−graphene due to an interplay of applied field and strain. We propose that such mechanisms, based on morphological changes, can serve as an explanation of experimentally observed switching[9] or as a possible way for a memory device fabrication with carbon chain-like structures.

RESULTS AND DISCUSSION

Chains with 7 and 8 carbon atoms bridging GNRs, spanning a reasonable nanoscale gap of about 1.2 nm, were investigated. GNR zigzag edges were chosen to be consistent with previous suppositions based on the calculation of formation energies.[11] Carbon chains not aligned with the GNR armchair direction are referred to as noncollinear chains (NCC) and those parallel to the armchair direction as collinear chains (CC). Structural models are shown in Figure 1a−c, where density functional tight-binding (DFTB) optimized morphologies show a cumulene-like structure for C7 with collinear chain (C7-CC) and polyyne-like structures for C8 with collinear chain (C8-CC) and C8 with noncollinear chain (C8-NCC) (see Table S1 in Supporting Information for bond length values), with BLA of 0.01, 0.15, and 0.14, respectively, consistent with previous results applying first-principles DFT.[23] Bond lengths of carbons at the end of the chain, bonded to the GNR, were lengthened due to sp^2 hybridization.[15] End effects in finite carbon chains were discerned theoretically, showing increased change of the BLA at the carbon atom chain end.[30] C8-CC was found to be lower in energy by about 5 kcal/mol compared to C8-NCC, which can be explained by lower stress exerted on the chain. DFTB results were in agreement with those we calculated with DFT[31] using the PBE functional (*ca.* 7 kcal/mol), thus establishing transferability of the TB parameters.

On the other hand, in optimizing the cumulenic C7-NCC nanodevice model system, a structural transformation resulting in a C4 carbon chain attached to a reconstructed pentagon with a dangling carbon atom evolved, possibly due to the lower stability of the cumulene-like structures,[16] with the C7-CC optimized structure higher in energy (*cf.* Figure 2, C4-NCC, C7-CC, 0% applied uniaxial strain, UAS, along the chain direction). The relative energies per atom indicated the C7-CC structure to be lower than C8-CC by 0.54 kcal/mol. Interestingly, in experimental atomic

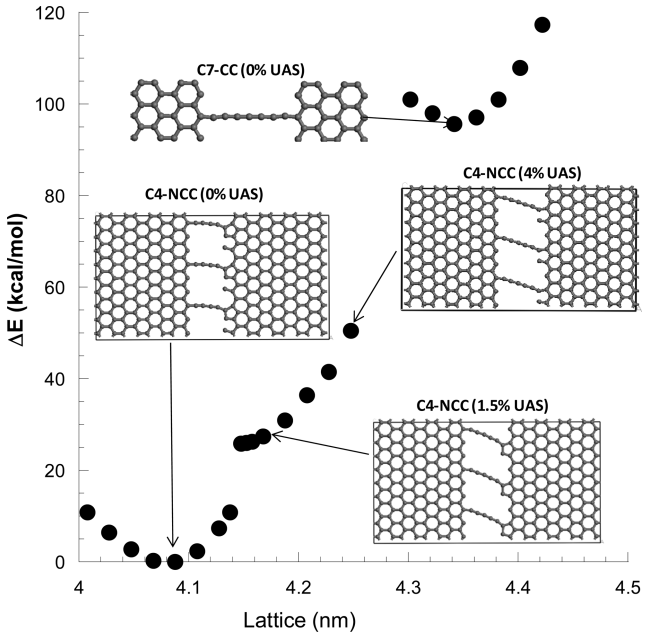

Figure 2. Energy change (ΔE) between conformations under uniaxial strain, relative to the value at 0% uniaxial strain (UAS), at 4.09 nm. For clarity, we show three unit cells along the transverse direction. Inset: curve shown was obtained at 0 K. To ascertain the stability of the structures, DFTB MD simulations for 1 ps at room temperature were further performed for C7-CC, and the structures were shown to stay stable.

resolution observations,[12] it was shown that constriction to single carbon chains upon electron irradiation resulted in stable morphologies that included pentagons, as well as higher polygons, and that atom rearrangement is an important factor in the reconstruction. In examining GNR neck-like structures formed upon the application of strain by first-principles MD simulations, similar structural reconstruction was observed.[32] At the same time, in the experimental work by Standely *et al.*,[13] it was demonstrated that, following electrical breakdown of graphene sheets to a carbon chain-like structure, application of appropriate bias voltage pulses led to reproducible switching in a robust nanodevice that persisted for more than 24 h. This observation could imply structural reorganization upon bias application, causing the switching.

We demonstrate on the basis of DFTB calculations that variation in the structural motif, for example, the formation of the pentagons at the interface of the chain−graphene, can readily be achieved *via* the application of UAS and bias or gate voltage. UAS of about 1.5% applied on the C4-NCC structure resulted in an opening of the pentagon to form a new one that is merged with the dangling carbon atom, originally present in the equilibrium structure (inset in Figure 2). The 1.5% strained structure is now a C5 chain attached to a pentagon. An increase in UAS of up to 4% opened the pentagon ring again, forming a C6 chain with a dangling carbon.

Furthermore, we investigated the stability of chains terminated with a pentagonal structural motif as it is formed or annihilated, as shown in the insets of Figure 3a,b, summarizing results of the energy path under UAS in extension or compression for the C7 and C8 chains, respectively. Each point in the graphs represents a full structural optimization under UAS at 0 K. As indicated, we started from a structure having a pentagon structural motif and applied extension up to about 6%. For both even and odd carbon chain models, the energy increased up to breakage of the pentagon (4% elongation), and thereafter, for the odd chain (C7), a transition from a five- to a four-membered ring structure occurred. For the even chain (C8), there was no ring formation. An increase to about 6% elongation caused breakage of the four-membered ring in the odd chain model, and the chain stretched to 9 carbon atoms. Upon compression, in the absence of an applied electric field, starting from the elongated structures at *ca.* 6%, the previous reconstructed structures (chain terminated with a pentagon) could not be recovered in either the odd or even chains. Instead, a four-membered ring was formed in the C7 chain, but no ring was formed for the C8 chain. However, we found that the reconstructed five-membered ring could readily be formed under an applied field, including application in the transverse direction, as elaborated on in the Supporting Information. These results are encouraging and suggest that the formation and annihilation of the rings at the interface of a carbon chain/graphene can be achieved *via* applied strain under bias or gate voltage.

To gain insight into the effects of strain on the electronic properties of the carbon chains bridged between GNRs, we carried out $I-V$ calculations using

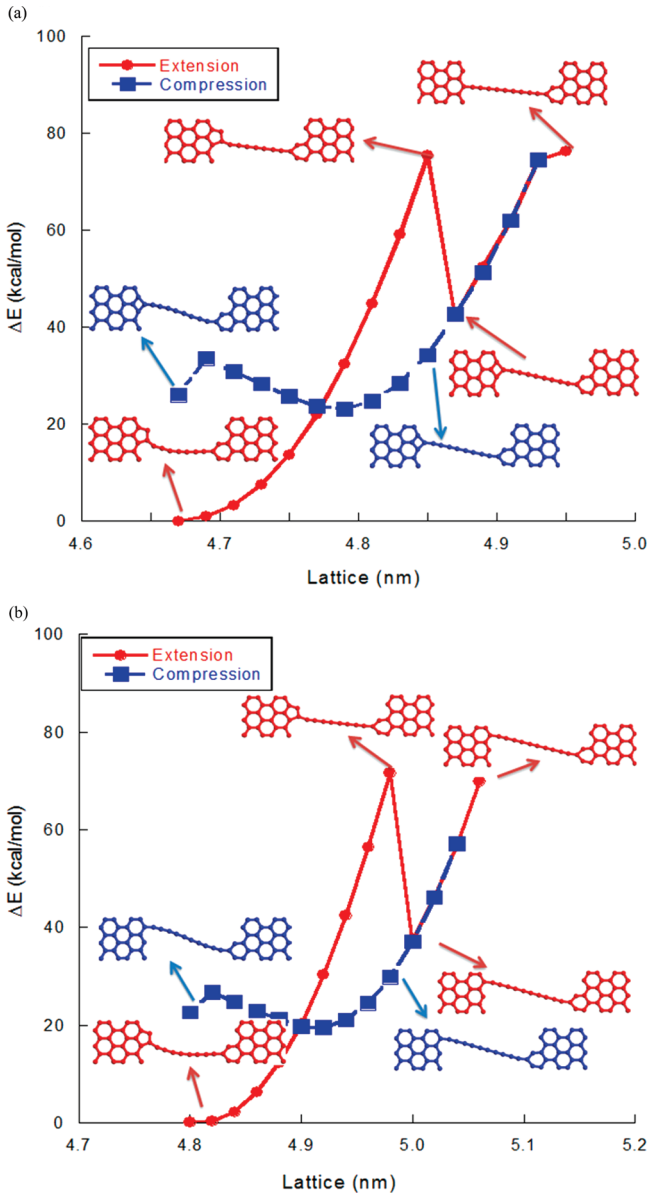

Figure 3. Energy (kcal/mol) relative to a structure having a pentagon structural motif (lattice constant 4.67 nm), as a function of an applied strain, for (a) odd carbon chain (C7) terminated by five- and six-membered rings, and (b) even chain (C8) terminated by five- and six-membered rings.

gDFTB,[33] a modified version of DFTB that includes the non-equilibrium Green's function formalism for the calculation of the transmission coefficients. The non-equilibrium implementation was carried out by the Meir−Wingreen equation,[34] considered to be a generalized formalism than Landauer−Buttiker.[35] A complete account of this method is given elsewhere.[36] The electron transport model adopted in this work is shown in Figure 1d, where the leads are made of GNRs to reduce the effects of the electrodes at the interface with the scattering region. Results of the *I*−*V* characteristics are summarized in Figure 4a,b. Comparing C7-CC and C8-CC, it is noted that the chain with an odd number of carbons exhibited a higher output current as compared to the even carbon chain. This difference can be explained by the cumulene-like *versus* polyyne-like electronic structure, respectively, because the cumulene structure is highly conductive. The application of small strains of about ±2% on C7-CC resulted in *ca.* 16% change in the output current, where compression (−2%) tended to increase the current while extension (+2%) decreased it. The low current obtained under extension may be explained by the lengthened bonds at the terminations of the chain, as it tends to separate from the sp^2 GNR structures under an applied strain and increase the BLA, while the opposite may happen upon compression. However, a detailed study of this behavior will be carried out in future work. Effects of applied strain on the *I*−*V* characteristics were also demonstrated for C4-NCC, as shown in Figure 4b, for 0, 1.5, and 4% UAS.

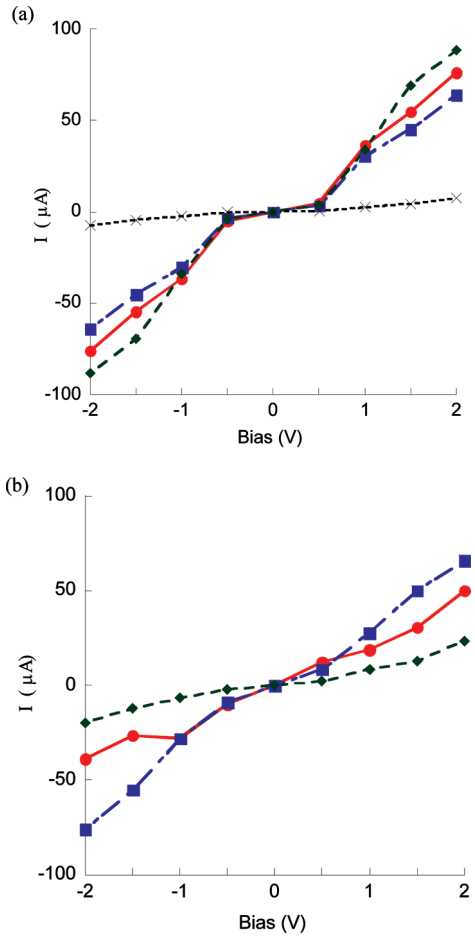

Figure 4. *I*−*V* characteristics for (a) C7-CC under UAS 0% (red circle); +2% (blue square); −2% (green diamond), C8-CC 0% (black asterisk); (b) C4-NCC under UAS 0% (red circle), 1.5% (blue square), 4% (green diamond).

The largest output currents were obtained under a reverse bias of −2 V. At zero strain, the equilibrium structure consisted of a C4 chain attached to a pentagon, with an output current of 40 (μA). The application of 1.5% strain transformed the structure to a C5 chain attached to a pentagon, doubling the output current to 80 (μA). A further application of 4% strain opened the pentagon ring, resulting in a new structure with a six-carbon atom chain and a dangling carbon. This resulted in a drop in the output current, as expected in chains with an even number of atoms. Asymmetry in the *I*−*V* curves can be attributed to asymmetry of the structures due to the morphological transformations.

We propose a switching device based on structural reconstruction at the interface of a carbon chain−graphene by an interplay of bias or gate and an applied strain. This mechanism may be used also to explain the experimental results obtained in ref 13. However, as realistic samples will be considered, optimal conditions for achieving such a device are yet to be determined experimentally.

CONCLUSIONS

We investigated effects of strain on carbon chains bridged between GNRs. Our calculations suggest that the chains tend to form collinearly, but noncollinear chains can be formed and are stable. Noncollinear chains with a reconstructed pentagon were found to undergo structural transformation under strain, driving the number of atoms in the chains from even to odd or *vice versa*. The formation of the pentagons is readily achieved *via* an applied bias or gate voltage and strain. The change in the number of atoms in the chain, due to the formation/annihilation of the rings at the interface of the carbon chain−graphene, leads to large fluctuations in the output current, an effect that can be used to fabricate switching nanodevices.

COMPUTATIONAL DETAILS

Calculations were carried out using density functional tight binding (DFTB)[37] method, known for its efficiency to handle large systems. The implementation of the self-consistent charge equilibration renders this method well-suited for the present work. Model structures were fully optimized within the self-consistent charge equilibration, using carbon parameters fitted to periodic systems (pbc-01).[38] Periodic boundary conditions (pbc) were applied in the longitudinal direction, as well as in the transverse direction to the chain (see Figure 1d) to permit examination of the intrinsic properties of the carbon chain in the nanodevice.

Calculations to investigate the reconstruction at the interface, using first-principles method, were performed with an all-electron DFT scheme implemented in DMol^3.[39] We employed the PBE[40] functional and a DNP basis set. Since DMol^3 does not allow for the application of an electric field in periodic systems, we used a superstructure, where the edge atoms of the nanoribbons were frozen during optimization to mimic an extended system.

Acknowledgment. The DoD High Performance Computing Modernization Program is gratefully acknowledged for computer time and the AFRL DSRC for helpful support. The authors wish to thank A. Pecchia for providing the gDFTB transport code.

Supporting Information Available: We provide bond lengths (Table S1) of the model structures shown in Figure 1, as well as first-principles results on the formation of a five-membered ring at the interface of a carbon chain−graphene structure under an applied field (Figure S1). This material is available free of charge *via* the Internet at http://pubs.acs.org.

REFERENCES AND NOTES

1. Burghard, M.; Klauk, H.; Kern, K. Carbon-Based Field-Effect Transistors for Nanoelectronics. *Adv. Mater.* **2009,** *21*, 2586–2600.
2. Martel, R.; Schmidt, T.; Shea, H. R.; Hertel, T.; Avouris, Ph. Single- and Multi-Wall Carbon Manotube Field-Effect Transistors. *Appl. Phys. Lett.* **1998,** *73*, 2447–2449.
3. Wind, S. J.; Appenzeller, J.; Martel, R.; Derycke, V.; Avouris, Ph. Vertical Scaling of Carbon Nanotube Field-Effect Transistors Using Top Gate Electrodes. *Appl. Phys. Lett.* **2002,** *80*, 3817–3819.

4. Novoselov, K. S.; Geim, A. K.; Morozov, S. V.; Jiang, D.; Zhang, Y.; Dubonos, S. V.; Grigorieva, I. V.; Firsov, A. A. Electric Field Effect in Atomically Thin Carbon Films. *Science* **2004,** *306*, 666–669.
5. Novoselov, K. S.; Geim, A. K.; Morozov, S. V.; Jiang, D.; Katsnelson, M. I.; Grigorieva, I. V.; Dubonos, S. V.; Firsov, A. A. Two-Dimensional Gas of Massless Dirac Fermions in Graphene. *Nature* **2005,** *438*, 197–200.
6. Geim, A. K.; Novoselov, K. S. The Rise of Graphene. *Nat. Mater.* **2007,** *6*, 183.
7. Geim, A. K. Graphene: Status and Prospects. *Science* **2009,** *324*, 1530–1534.
8. Castro Neto, A. H.; Guinea, F.; Peres, N. M. R.; Novoselov, K. S.; Geim, A. K. The Electronic Properties of Graphene. *Rev. Mod. Phys.* **2009,** *81*, 109–162.
9. Xia, F.; Farmer, D. B.; Lin, Y.-M.; Avouris, P. Graphene Field-Effect Transistors with High On/Off Current Ratio and Large Transport Band Gap at Room Temperature. *Nano Lett.* **2010,** *10*, 715–718.
10. Wang, X; Ouyang, Y.; Li, X.; Wang, H.; Guo, J.; Dai, H. Room-Temperature All-Semiconducting Sub-10-nm Graphene Nanoribbon Field-Effect Transistors. *Phys. Rev. Lett.* **2008,** *100*, 206803.
11. Jin, C.; Lan, H.; Suenaga, K.; Iijima, S. Deriving Carbon Atomic Chains from Graphene. *Phys. Rev. Lett.* **2009,** *102*, 205501.
12. Chuvilin, A.; Meyer, J. C.; Algara-Siller, G.; Kaiser, U. From Graphene Constrictions to Single Carbon Chains. *New J. Phys.* **2009,** *11*, 083019.
13. Standley, B.; Bao, W.; Zhang, H.; Bruck, J.; Lau, C. N.; Bockrath, M. Graphene-Based Atomic-Scale Switches. *Nano Lett.* **2008,** *8*, 3345–3349.
14. Tammann, G. Z. Carbon Formed by the Action of Mercury on Carbon Tetrachloride, Carbon Tetrabromide and Carbon Tetraiodide. *Anorg. Allg. Chem.* **1921,** *115*, 145–158.
15. Ravagnan, L.; Manini, N.; Cinquanta, E.; Onida, G.; Sangalli, D.; Motta, C. Effect of Axial Torsion on sp Carbon Atomic Wires. *Phys. Rev. Lett.* **2009,** *102*, 245502.
16. Gu, X.; Kaiser, R. I.; Mebel, A. M. Chemistry of Energetically Activated Cumulenes—From Allene (H_2CCCH_2) to Hexapentaene ($H_2CCCCCCH_2$). *Chem. Phys. Chem.* **2008,** *9*, 350–369.
17. Hu, Y.-H. Stability of sp Carbon (Carbyne) Chains. *Phys. Lett. A* **2009,** *373*, 3554–3557.
18. Kim, S. Synthesis and Structural Analysis of One-Dimensional sp-Hybridized Carbon Chain Molecules. *Angew. Chem., Int. Ed.* **2009,** *48*, 7740–7743.
19. Borrnert, F.; Borrnert, C.; Gorantla, S.; Liu, X.; Bachmatiuk, A.; Joswig, J.-O; Wagner, F. R.; Schaffel, F.; Warner, J. H.; Schonfelder, R.; *et al.* Single-Wall-Carbon-Nanotube/Single-Carbon-Chain Molecular Junctions. *Phys. Rev. B* **2010,** *81*, 085439.
20. Lang, N. D.; Avouris, Ph. Oscillatory Conductance of Carbon-Atom Wires. *Phys. Rev. Lett.* **1998,** *81*, 3515–3518.
21. Deng, X.; Zhang, Z.; Zhou, J.; Qiu, M.; Tang, G. J. Length and End Group Dependence of the Electronic Transport Properties in Carbon Atomic Molecular Wires. *J. Chem. Phys.* **2010,** *132*, 124107.
22. Tongay, S.; Senger, R. T.; Dag, S.; Ciraci, S. *Ab-Initio* Electron Transport Calculations of Carbon Based String Structures. *Phys. Rev. Lett.* **2004,** *93*, 136404.
23. Khoo, K. H.; Neaton, J. B.; Son, Y. W.; Cohen, M. L.; Louie, S. G. Negative Differential Resistance in Carbon Atomic Wire−Carbon Nanotube Junctions. *Nano Lett.* **2008,** *8*, 2900–2905.
24. Yuzvinsky, T. D.; Mickelson, W.; Aloni, S.; Begtrup, G. E.; Kis, A.; Zettl, A. Shrinking a Carbon Nanotube. *Nano Lett.* **2006,** *6*, 2718–2722.
25. Chen, W.; Andreev, A. V.; Bertsch, G. F. Conductance of a Single-Atom Carbon Chain with Graphene Leads. *Phys. Rev. B* **2009,** *80*, 085410.
26. Heyd, R.; Charlier, A.; McRae, E. Uniaxial-Stress Effects on the Electronic Properties of Carbon Nanotubes. *Phys. Rev. B* **1997,** *55*, 6820–6824.
27. Yang, L.; Anantram, M. P.; Han, J.; Lu, J. P. Band-Gap Change of Carbon Nanotubes: Effect of Small Uniaxial and Torsional Strain. *Phys. Rev. B* **1999,** *60*, 13874–13878.
28. Yang, L.; Han, J. Electronic Structure of Deformed Carbon Nanotubes. *Phys. Rev. Lett.* **2000,** *85*, 154–157.
29. Alam, K. Uniaxial Strain Effects on the Performance of a Ballistic Top Gate Graphene Nanoribbon on Insulator Transistor. *IEEE Trans. Nanotechnol.* **2009,** *8*, 528–534.
30. Fan, X.; Liu, L.; Lin, J.; Shen, Z.; Kuo, J.-L. Density Functional Theory Study of Finite Carbon Chains. *ACS Nano* **2009,** *3*, 3788–3794.
31. Delley, B. An All-Electron Numerical Method for Solving the Local Density Functional for Polyatomic Molecules. *J. Chem. Phys.* **1990,** *92*, 508–517.
32. Hobi, E., Jr.; Pontes, R. B.; Fazzio, A.; da Silva, A. J. R. Formation of Atomic Carbon Chains from Graphene Nanoribbons. *Phys. Rev. B* **2010,** *81*, 201406.
33. Pecchia, A.; Di Carlo, A.; Gagliardi, A.; Sanna, S.; Frauenheim, T.; Gutierrez, R. Incoherent Electron−Phonon Scattering in Octanethiols. *Nano Lett.* **2004,** *4*, 2109–2114.
34. Meir, Y.; Wingreen, N. S. Landauer Formula for the Current through an Interacting Electron Region. *Phys. Rev. Lett.* **1992,** *68*, 2512–2515.
35. Landauer, R. *IBM J. Res. Dev.* **1957,** *1*, 223.
36. Reimers, R. J.; Solomon, C. G; Gagliardi, A.; Bilic, A.; Hush, S. N.; Frauenheim, T.; Di Carlo, A.; Pecchia, A. The Green's Function Density Functional Tight-Binding (gDFTB) Method for Molecular Electronic Conduction. *J. Phys. Chem. A* **2007,** *111*, 5692–5702.
37. Frauenheim, T.; Seifert, G. G.; Elstner, M.; Niehaus, T.; Koeler, C.; Amkreutz, M.; Sternberg, M.; Hajnal, Z.; Di Carlo, A.; Suhai, S. Atomistic Simulations of Complex Materials: Ground-State and Excited-State Properties. *J. Phys.: Condens. Matter.* **2002,** *14*, 3015–3047.
38. http://www.dftb.org.
39. Delley, B. From Molecules to Solids with the DMol3 Approach. *J. Chem. Phys.* **2000,** *113*, 7756–7764 (implemented by Accelyrs Inc.).
40. Perdew, J. P.; Burke, K.; Ernzerhof, M. Generalized Gradient Approximation Made Simple. *Phys. Rev. Lett.* **2006,** *77*, 3865–3868.